COMPUTATIONAL METHODS FOR BALL BEARINGS IN SPACECRAFT

M J Todd

European Space Tribology Laboratory, UKAEA, UK

Abstract

The rolling resistance (torque) and thermal conductance of ball bearings are often of great concern in the design of spacecraft mechanisms. These properties can show large variations where thermal gradients exist, particularly so in structures which are not iso-expansive.
If, as is frequently the case, viscous losses can be ignored, then the remaining "dry" or Coulomb frictional torque may be estimated from a simple theoretical model first proposed at ESTL in which microslip, hysteresis and spin are assumed to act independently. With the limitation that the load-carrying proportion of the ball complement is not predictable and therefore an assumption is necessary, this model gives computed results which are usefully close to practice.
Thermally imposed strains and the mitigating effect of structure compliance can be quickly assessed by iteration methods on the computer, which allows design or material changes to be optimised.
Examples show the usefulness of computer-assisted design study on actual mechanisms.
Bearing misalignment, because of moment loading for example, can result in torque anomalies from ball speed /position variation. Whilst no complete torque prediction treatment exists (there are many influencing factors) it is still useful to be able to compute ball speed /position variation as a function of degree of misalignment. The method of doing this is outlined.
The heat conductance across a dry Hertzian contact area has been observed to be proportional to the area itself. Thus the dry conductance for a ball bearing can be easily computed and used as a worst case value in thermal modelling of the mechanism.

1 Introduction

The ball bearing is an economical and efficient means of supporting rotational structures in spacecraft. Because it has high internal stiffness, however, it is sensitive to any thermal or mechanical strains which the surrounding structure might impose. Therefore it is often important to be able to assess what consequences such strains will produce.
This paper is concerned with how ball load, contact angle, dry frictional torque, ring deflection, ball speed/position variation and thermal conductance can be computed from a mixture of rolling contact theory, experimental measurement and a few empirically-based assumptions.

2 Computation of contact angle and ball load

Let us first suppose, as is almost always the case in spacecraft mechanisms, that we have an axially preloaded pair of angular contact bearings which have to support a rotating shaft and are fitted to an external housing. (The four-point contact bearing used in some mechanisms can be regarded as effectively a preloaded pair of angular contact bearings with zero ring separation).

2.1 Preloading (axial loading)

The initial act of preloading, either to a defined axial load or to a defined axial interference, will produce a change (increase) of contact angle and a concomitant increase in normal ball load.
We could also postulate "negative" preloading, or axial clearance, where there would be a notional decrease in angle and a reduction of ball load. However we will consider here only positive preloading.
Fig. 1 shows the positions of the raceway centres of curvature before and after positive axial preloading by a force F_a. The separation AB of the centres of curvature are exaggerated in this and subsequent Figs. for the sake of clarity. From conventional Hertz deformation theory (for example Harris,1966) combined with the geometry of Fig.1 we have (for symbol meanings, see nomenclature):

$$\frac{F_a}{Z.K_n\ (AB)^{3/2}} = \sin\alpha_p \left(\frac{\cos\alpha}{\cos\alpha_p} - 1 \right)^{3/2} \quad \ldots .\ 1$$

$$Q_p \equiv K_n\, \delta_{np}^{\ 3/2} = K_n \left[AB \left(\frac{\cos\alpha}{\cos\alpha_p} - 1 \right) \right]^{3/2} \quad \ldots .2$$

Proceedings of the First European Symposium on 'Space Mechanisms & Tribology', Neuchâtel, Switzerland, 12-14 Oct. 1983. (ESA SP-196, publ. December 1983).

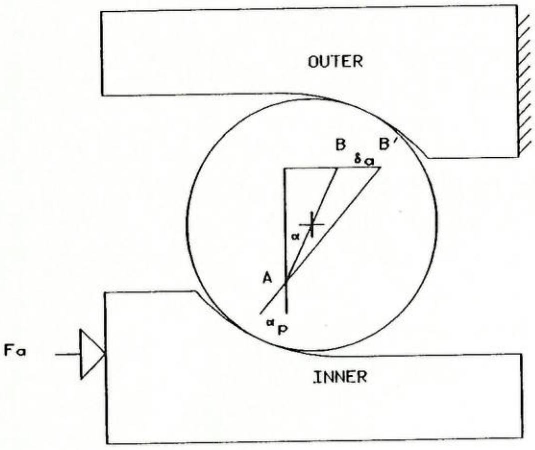

Figure 1. Axial preloading before fitting (A and B are the original outer and inner centres of curvature).

The Hertz constant k_n may be closely approximated by the very useful regression formulae given by Brewe and Hamrock (1977) which avoids the computation of elliptic integrals (see Appendix). The contact angle, α_p after preloading, may be found by iterative solution of eq.1 to a predetermined accuracy. The ordinary single variable Newton Raphson method is easily programmed and rapidly convergent.

2.2 Fitting

If the preloaded bearings are then interference fitted to their seatings at either inner or outer rings then this action will change both the contact angle and the normal ball load.
Where the radial compliance of the shaft or housing cannot be assumed zero then it is necessary to use "thick ring" theory to calculate the radial movement of the inner and outer ring centres of curvature. Expressions for these radial movements are given by Harris(1966) and are easily converted into software.

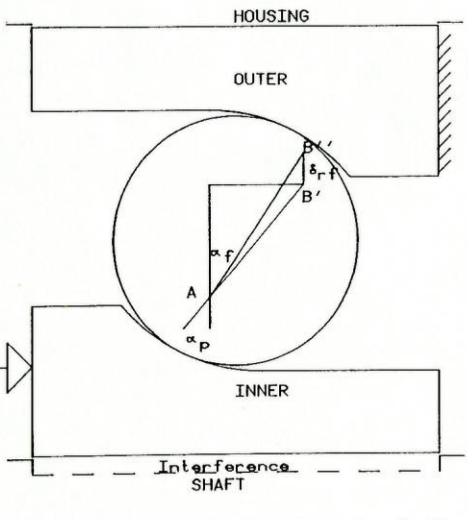

Fig.2 Preloaded bearing after fitting to shaft

Let us designate δ_{rf} as the radial ring shift, due solely to fitting, of the inner ring centre of curvature relative to the outer ring centre, which we may for convenience assume to be fixed.
Then, as will be seen in Fig.2, the new contact angle is given by:

$$\tan \alpha_f = \frac{AB' \sin \alpha_p}{\delta_{rf} + AB' \cos\alpha_p} \qquad ....3$$

And the extra Hertz normal approach due to fitting is:

$$\delta_{nf} = AB'\left(\frac{\sin \alpha_p}{\sin \alpha_f} - 1\right) \qquad ....4$$

whence the total normal ball load, after preloading and fitting will be:

$$Q_p + Q_f = K_n \, (\delta_{np} + \delta_{nf})^{3/2} \qquad ....5$$

Note here that since a strain is imposed by interference fitting, we may calculate the effect on contact angle and on ball load directly without iteration.
If the preloading is "hard",ie. the axial compliance of the device used for preloading is small compared with the Hertzian axial compliance of the bearings, then the above equations are directly applicable. However, where there is a preload compliance present then fitting would cause an axial displacement or relief of the rings to bring about a balance between the force exerted by the preloading device and the axial force from the loaded ball set (we assume, of course, that such an axial relief is possible by virtue of a clearance between one of the rings and the structure).

2.3 Thermal strain

Thermal expansion or contraction of the bearing rings and of the surrounding structure will further introduce relative axial and radial shifts of the rings and therefore will change both contact angle and ball load.
The radial shift will be a result of both ring expansivity and of the change in interference caused by any difference in expansivity between ring and structure.
The axial shift will depend upon the structural and spacing materials and upon the axial compliance of these materials as well as upon the compliance of the preloading method.

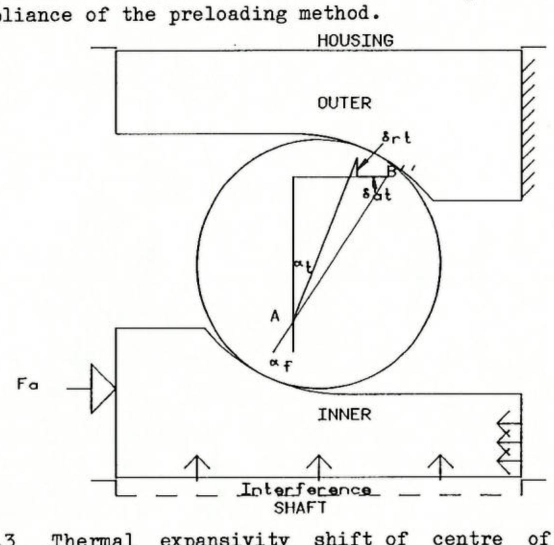

Fig.3 Thermal expansivity shift of centre of curvature (outer ring assumed fixed for clarity)

From Fig. 3, letting δ_{at} be the axial thermal shift, δ_{rt} the radial thermal shift due both to ring expansion and interference change then we have:

$$\tan \alpha_t = \frac{\delta_{at} + AB'' \sin \alpha_f}{\delta_{rt} + AB'' \cos \alpha_f} \quad \ldots .6$$

and the normal approach due to thermal changes is:

$$\delta_{nt} = \sqrt{(AB'' \cos \alpha_f + \delta_{rt})^2 + (AB'' \sin \alpha_f + \delta_{at})^2} - AB'' \quad \ldots .7$$

The resulting total normal ball load, where there is a hard preload and structure, is:

$$Q \equiv Q_p + Q_f + Q_t = K_n (\delta_{np} + \delta_{nf} + \delta_{nt})^{3/2} \quad \ldots .8$$

When either the preload device or the structure is "soft" then again there will be axial relief of the rings to cause a balance between internal and external forces on the bearing.
In this case the value of δ_{at} in the above equations would be changed by the amount of axial ring shift and one would again use iteration (Newton Raphson) to determine the effective value which gave a balance of axial forces. A change in contact angle and ball load would of course result from this axial shift.
If both inner and outer rings are constrained in a compliant way then it is necessary to employ the two variable Newton Raphson method since there would then be two unknowns, viz. the inner and outer ring axial shifts. However, it is rare in practice to have soft structures combined with soft preload.

Nomenclature

Symbol	Meaning
Fa	Axial force (preload)
Z	Ball complement
k_n	Hertz deflection constant
$\alpha, \alpha_p, \alpha_f, \alpha_t$	Ball contact angle
α'	Hysteresis loss coefficient
δ_n	Hertzian normal approach (subscripted p,f or t)
Q, Qp,Qf,Qt	Ball normal load
AB	Centres separation (Fig. 1)
AB'	AB.cos α /cos α_p (Fig.1,2)
AB''	AB'.sin α_p /sin α_f (Fig.2,3)
Tm,Th,Ts	Frictional torque
μ	Sliding friction coeff.
D	Ball diameter
dm	Bearing pitch circle diam.
β	Microslip parameter $=4a^2/(\mu p_o E'D^2)$
p_o	Maximum Hertz pressure
a	Ellipse semi-major axis
k	Ellipticity (ratio of axes)
E1	Elliptic integral(1st kind)
E2	Elliptic integral(2nd kind)
E	Young's modulus
σ	Poisson's ratio
E'	Material constant $=2/((1-\sigma_A^2)/Ea+(1-\sigma_B^2)/Eb)$
C	Ball conformity (ratio of race to ball radius)
R	1/Rx + 1/Ry (see Appendix)

3.1 Torque model

For those spacecraft ball bearings where solid lubricants are used or where minimal liquid lubrication (and/or low speed) makes viscous effects negligible, the torque will be caused by solid friction and will be load-dependent. Therefore, from the above section, thermal or mechanical strains, because they affect ball load and contact angle, will also influence the torque. The three processes contributing to frictional rolling resistance of a ball in a groove are microslip, hysteresis and ball spin.
In reality these processes combine within the bearing in a complex interaction and some simplification is always necessary to yield tractable solutions.
A simple and easily calculated Coulomb torque model has been proposed (Todd,1980) which makes the following assumptions:

1. the ball rolls without spin at one raceway contact and spins bodily as it rolls at the other contact;
2. microslip occurs only at the pure rolling contact whereas hysteresis loss occurs at both ball contacts;
3. the sliding friction coefficient between ball and raceway is independent of contact stress and of rolling velocity;
4. the net torque of the bearing is the additive combination of the microslip, hysteresis and spin components.

3.2 Numerical expressions for torque components

3.2.1 Microslip

Based upon the elemental strip theory of the motion of a ball rolling in a groove (Johnson,1962) the rolling resistance Fm and the corresponding torque Tm, per ball, can be closely approximated by the following formulae :

$$T_m = 0.08\mu \frac{Q}{D^2} . a^2 (1 - 0.5e^{-(\beta - 10)/25}) . (d_m \pm D\cos\alpha) \quad \ldots .9$$

for $\beta > 10$

$$\text{or } T_m = 0.0078\beta^{0.695} \frac{\mu Q}{D^2} a^2 (dm \pm D\cos\alpha) \quad \ldots .10$$

for $0 < \beta \leq 10$

Where:upper sign is for inner raceway, lower is for outer.

For most conventional ball bearings β is greater than 10 and so the upper equation would apply. Values for the ellipse dimensions (a and k) and for the maximum Hertz pressure po (required for the calculation of β) may be found from the useful formulae given in the Appendix .

3.2.2 Hysteresis

From the elastic hysteresis of sub-surface material in rolling, the energy loss given by Tabor (1955) yields the following contribution to bearing torque:

$$T_h = \frac{H\,a\,\alpha'\,Q}{4\,kD}\,(d_m \pm D\cos\alpha) \qquad \ldots.11$$

The value to be used for H is approximately $4/3\,\pi$ for conforming ball/groove contacts and the value of α' is ca. .01 for hard steels.

3.2.3 Spin

The torque required to cause spin of a ball about the normal to the Hertzian contact area may be easily derived from the Hertzian pressure distribution. From this spin torque the resultant bearing torque is:

$$T_s = \frac{3\mu Q a E_2 \sin\alpha}{8} \qquad \ldots.12$$

Where E2 is the elliptic integral of the second kind, found conveniently from the Appendix formula.

3.2.4 Total Coulomb torque

Following the above model we add the torque components from each ball. The ball spin torque, which is usually the dominant term, is first evaluated at each raceway. Spin is assumed to occur at that raceway for which the spin torque is lower.

3.3 Non-calculable quantities required for torque estimate

Following the above model there are three empirically derived inputs necessary before torque can be computed. These are the sliding friction coefficient, μ the hysteresis loss coefficient, α' and the number of balls, Z, assumed to be effectively sharing the load.

The range of sliding coefficient for solid- or boundary lubricated contacts is quite small. Values from 0.1 to 0.2 are measured for solid films and for most compatible oils and greases. For a particular lubricant the variation of this coefficient is however quite large, of the order 25% (3 sigma level) and thus the computed torque, since it is almost linearly proportional to friction coefficient, is subject to a similar error.

The hysteresis loss coefficient for hard bearing steel is approximately 0.01 and since the hysteresis term is generally a small fraction (less than 10%) of the total then the assumed coefficient is not critical.

The number of balls assumed to be load-carrying depends very much upon the size and ball complement, the original bearing precision, the mounting precision, flexure of rings under load and so on. Whereas for small, high precision bearings with fewer than about 15 balls the effective ball complement can be taken as the actual complement, this is not the case for large, many-ball bearings, particularly where precision might be lower or where a thin ring design with flexible rings is being used (as, for example, the four-point contact type fitted to the BAE APM design). For such bearings it is necessary to adopt a "rule of thumb" approach based upon experimental data. (Fortunately, the torque varies only as the reciprocal of the cube root of Z, so the sensitivity is not high).

3.4 Correlation of torque model prediction with measurement

3.4.1 Mechanically loaded bearings

From measured Coulomb torque of axially loaded ball bearings of various types, in sizes from 4mm to 98mm OD, good agreement has been found with the torque model outlined above. Some early examples are given by Todd (1980) with the parameters of ball complement and ball-to-groove conformity. In the case of 42-ball bearings the torque was well matched by assuming only 10 balls (ie. approximately 1/4 of the full ball complement) actually carried the load.

3.4.2 Thermally loaded bearings

To simulate the more directly relevant situation of radial thermal gradients across ball bearings, the dry torque has recently been measured at ESTL of a bearing pair of the type and size to be used in the BAE L-SAT Solar Array Drive Mechanism (SADM). Temperature differences from shaft to housing of some 20 or 30 deg C are expected in orbit. The bearings are dry lubricated with ion-plated lead film whose sliding friction coefficient is 0.15±0.05 (3 sigma level).

In this design it was important to know how thermal gradients affected the torque of the bearings and specifically to choose a preload compliance which gave a compromise, ie. was low enough to avoid excessive vibrational amplitudes (resonance) during launch and yet high enough to prevent undue variations of thermally induced loads during operation in orbit.

For the case of a ferritic steel structure and spacer, the measured mean torque for four different compliances of preload are plotted in Figs. 4 to 7 together with the computed torque.

FIG.4 Torque(g.cm)vs.Outer Ring Temp.(C)

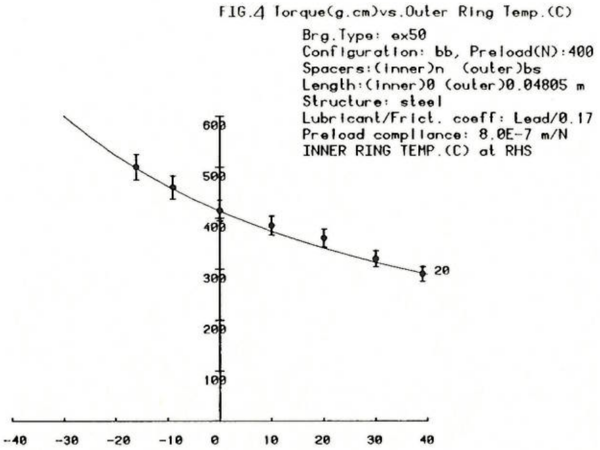

FIG.5 Torque(g.cm)vs.Outer Ring Temp.(C)

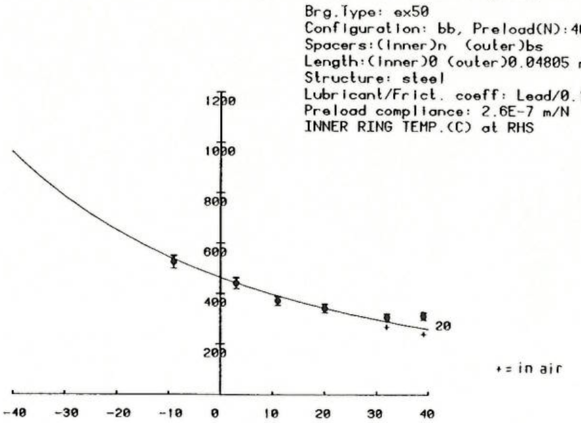

FIG.7 Torque(g.cm)vs.Outer Ring Temp.(C)

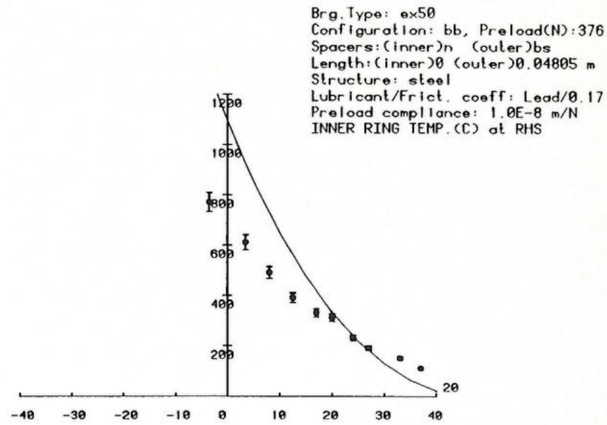

FIG.6 Torque(g.cm)vs.Outer Ring Temp.(C)

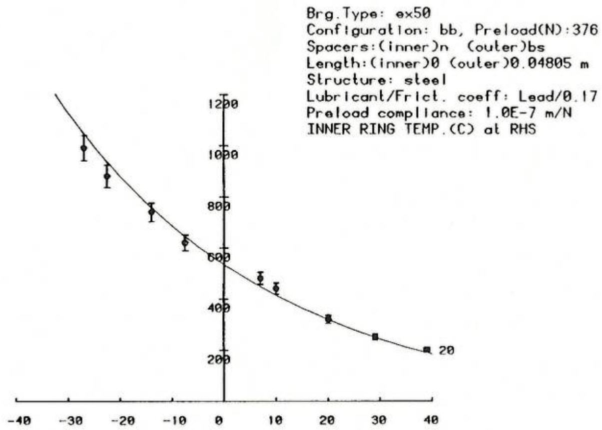

The experimental points are shown superimposed upon digitally plotted curves from a computer program incorporating the formulae of Sections 2 and 3. The details of each condition are shown in the Figs.

As the preload compliance becomes progressively lower (ie. harder preloading) from Fig. 4 to Fig.7 it is seen that the torque variation increases. In each case the axial compliances were measured values and the effective friction coefficient of the lead film was deduced by matching the computed torque to the observed torque at the 20C/20C point only. The value used for all plots was 0.17 which is within the range quoted above. (A load cell gave the axial preload in the bearings as they were thermally cycled). There is good agreement within experimental scatter of the measured torque for all compliances except for the smallest compliance where the divergence is probably because of errors in the measured compliance.

Almost complete offloading (torque falling towards zero) occurred with this lowest compliance, so a higher preload compliance would be necessary to avoid that consequence. The compliance actually chosen by BAE was approximately that of Fig.5.

The result of substituting an aluminium alloy housing for the ferritic steel housing is shown in Fig. 8 in which the conditions are otherwise identical with those of Fig.5 .

Here we see a steeper variation in torque (than in Fig. 5) when the housing is cooler than the shaft because of the greater radial strain from the aluminium.

Most of the above torque data were obtained with a heat- conducting grease between the rings and their seatings.

An interesting effect is shown in Figs 5 & 8 which compare the torque in vacuum (of less than 0.01 torr, ie. with no conduction or convection possible) with that in laboratory air when the heat-conducting grease had been removed. Where the housing (outer ring) is warmer than the shaft there is a noticeable departure from the theoretical curve in the in-vacuum case. This is believed to be due to the poorer heat transfer between housing and outer ring, which causes the outer ring to be cooled by conduction through the ball contacts to a temperature significantly below the housing temperature. In consequence the torque does not fall as predicted on the simple assumption that the ring temperature is the same as the housing temperature. On the other hand, with the housing cooler than the shaft, the torque does closely follow the prediction, even in vacuum and with no heat-conducting grease because there is then good heat transfer between housing and ring (by virtue of the housing being slightly cooler than the outer ring).

This discrepancy serves to show the limitations of the present computer analysis in the face of reality! Of course it would be desirable to refine the predictions by performing a preliminary thermal node analysis to estimate the true ring temperatures but, unfortunately, the uncertainties in emissivity, contact conductance etc. could mean significant error in the estimated nodal temperatures. However, from the design point of view it would usually be preferable to accept the cruder analysis (rings assumed isothermal with structure) as a worst case.

4 Deflection and misalignment in bearings under general loading

Numerous possible causes exist for relative ring misalignment: radial or moment loads, ring seating squareness errors, lack of co-axiality between bearing axes, ring flexure, axial asymmetry of temperature distribution and so on.

In the almost ubiquitous angular contact bearing used in spacecraft mechanisms the most important result of misalignment is the phenomenon of ball speed variation (BSV) and its corollary, ball position variation(BPV). These are caused by the

changes of contact angle, on which the orbital velocity of each ball depends, as the ball moves around the bearing. If the amount of BPV is low, ie. small compared with the latitude afforded to a ball by cage pocket or cage-to-land clearance, then there are no serious consequences. As misalignment increases, the cage is subject to circumferential loads because of the BPV. Such loads may result in cage wear or in severe cases in cage fracture and sudden failure.
This problem has been known for a long time (it is reviewed by Barish, 1968 who refers to a 1920's design to combat it).
The consequence of non-trivial BPV is the familiar cage "hang-up" effect on the bearing torque which is characterised by large low frequency peaks.
It is not possible to quantify the torque variation which a given amount of misalignment will cause since there are several influencing factors, such as: cage compliance, preload compliance, creep or slip under traction forces, besides of course ball/cage pocket and ring/cage clearances. However it is possible to compute quite simply the amount of BSV or BPV in a bearing and then to judge whether torque or cage wear problems are likely.
To calculate BSV or BPV one must first know the ring deflections and contact angles.
The general equations given by Jones (1960) for determining ring deflection, ball loads and contact angles constitute an iterative method which finds the net forces on each ball in equilibrium.
A small desk top computer will easily handle the iteration program provided that a relatively small number of bearings are involved - as is usually the case in spacecraft devices.
A detailed derivation of the governing equations is lengthy but straightforward and is given by Harris (1966). Since in the case of arbitrary vector loading there are three unknowns per bearing viz. axial, radial and angular deflection then one has to solve three simultaneous equations for each bearing. To do this by the iterative method for each bearing, the familiar Newton Raphson method, this time for three unknowns, is formed from the three simultaneous equations to produce three corresponding equations with the errors in the variables as the unknowns. From an initial guess of the three variables (deflections), iteration leads to convergence to a defined residual error. For m such bearings there would be 3m equations at most.
As a simplified example let us suppose we have a single, axially preloaded angular contact bearing and we apply a given moment load about an axis lying in the centre plane of the bearing.
From a computer program following the above iteration method, our example produces the print-out of Fig.9 which shows the bearing input data, the loads applied and the calculated deflections. Below these are tabulated the ball load, contact angle at each ball station. These values are computed from the ring deflections already evaluated. Then from the contact angles the ball speed and finally the ball position error (BPV) are tabulated.
The example, adapted from a real situation, also serves to illustrate the effect of ball/race conformity upon the amount of BSV and BPV. In the upper part of Fig.9 a bearing with a high conformity number (low conformity), though having a larger angular deflection (0.197 degrees) than that of the high conformity bearing in the lower

FIG.8 Torque(g.cm)vs.Outer Ring Temp.(C)

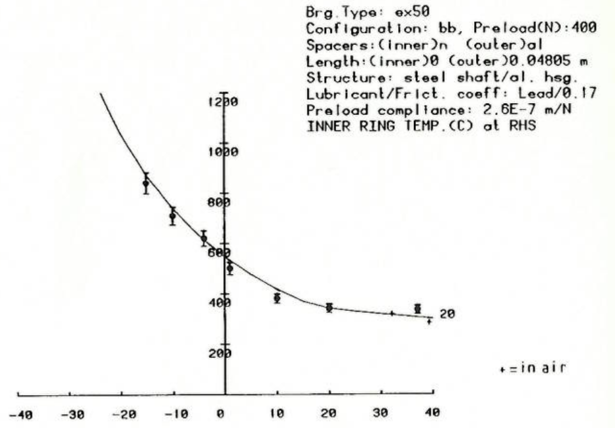

Ball loads and deflections of single brs.loaded axially, radially and with moment about a diameter
Ball diam.(m): 0.00714
PCD (m): 0.031
Nominal contact angle (deg): 15
Average conformity: 1.14
Ball complement: 10
RING MATERIAL:bs
BALL MATERIAL: bs

Axial load(N)	Radial load(N)	Moment load(Nm)
100	0	0.2

AXIAL DEFLECTION(M)= 1.02E-005
RADIAL DEFLECTION(M)= -1.53E-005
ANGULAR DEFLECTION(DEG)= 1.97E-001

BALL LOAD (N)	CONTACT (DEG)	AZIMUTH (DEG)	BALL SPEED (% OF MEAN)	POS'N ERROR MICRON
51	18.82	0	100.47	0
41	18.20	36	100.37	41
27	16.57	72	100.12	65
27	14.55	108	99.84	63
40	12.92	144	99.64	38
50	12.30	180	99.57	0
40	12.92	216	99.64	-39
27	14.55	252	99.84	-64
27	16.57	288	100.12	-66
41	18.20	324	100.37	-42

Ball loads and deflections of single brs.loaded axially, radially and with moment about a diameter
Ball diam.(m): 0.00714
PCD (m): 0.031
Nominal contact angle (deg): 15
Average conformity: 1.04
Ball complement: 10
RING MATERIAL:bs
BALL MATERIAL: bs

Axial load(N)	Radial load(N)	Moment load(Nm)
100	0	0.8

AXIAL DEFLECTION(M)= 1.24E-006
RADIAL DEFLECTION(M)= -1.29E-005
ANGULAR DEFLECTION(DEG)= 1.75E-001

BALL LOAD (N)	CONTACT (DEG)	AZIMUTH (DEG)	BALL SPEED (% OF MEAN)	POS'N ERROR MICRON
87	25.04	0	101.53	0
49	23.19	36	101.14	128
6	18.30	72	100.25	195
5	12.18	108	99.42	179
45	7.28	144	98.99	101
80	5.44	180	98.88	-4
45	7.28	216	98.99	-109
5	12.18	252	99.42	-187
6	18.30	288	100.25	-203
49	23.19	324	101.14	-136

FIG. 9

part (0.175 degrees),nevertheless has very considerably less BSV and BPV as seen from the two right hand columns of each table. The reason for this is that there is much less variation of contact angle in the low conformity bearing.
Since in conventional high precision bearings a typical ball position latitude within the cage pocket is 2% of ball diameter (in the bearings of Fig. 9 this latitude is therefore 143 microns) then no significant effect of the BPV in the low conformity bearing would be expected: whereas since the BPV in the high conformity case is much greater than the ball latitude then one would expect ball/cage interaction. Thus in the second case substantial torque fluctuations should probably occur.
This was indeed observed experimentally in duplex pairs of these same two conformities and with misalignment imposed by thin shims.
The foregoing treatment is therefore useful in indicating where there might be a problem with torque variation. It may be extended to deal with several bearings mounted in a shaft/housing structure which cannot be assumed rigid with respect to the bearings. In such cases the iterative procedure must balance the forces and moments induced in the bearings with those deforming the structure.

5 Thermal conductance

Measured values of radial thermal conductance in vacuo across ball bearings under known axial load (Stevens and Todd,1980) show that, whilst speed and oil quantity produce complex variations, the conductance across dry or solid-lubricated contacts follows a rather simpler relationship. This is that the conductance is linearly proportional to the area of elastic contact between each ball set and the raceway (after allowing for a small "zero-load" term which is largely due to radiative heat transfer).
To obtain an estimate, therefore, of the "dry" conductance it is necessary only to compute the (average) Hertzian contact area at the raceways end at the particular ball loads which exist. Any liquid lubricant present would usually give increased conductance because of the heat flow through the meniscus surrounding the ball but the presence of the ehl film complicates the situation and a general algorithm for computing conductance has not yet been formulated.
However if, as is often the case, a pessimistic, ie. low, estimate of heat conductance is preferred then the dry conductance alone would give it.
The conductance curve shown in Fig. 10 was obtained from a thermally stressed four-point contact bearing (Rowntree,1983) and show a fair match with computed values on the assumption, referred to above, that only ca. 1/4 of the ball complement(87) is load-carrying. With this same fraction assumed there was good correlation also with the measured Coulomb torque.

6 Conclusion

It has been shown in this brief review that many of the properties of ball bearings, intended for duty in spacecraft mechanisms, can be computed from standard theory with the aid of computer-modelling and a few empirically based assumptions. Because of the frequent presence of temperature differences across mechanism bearings it can be, and has proved, particularly useful to be able to quantify the thermal consequences upon ball

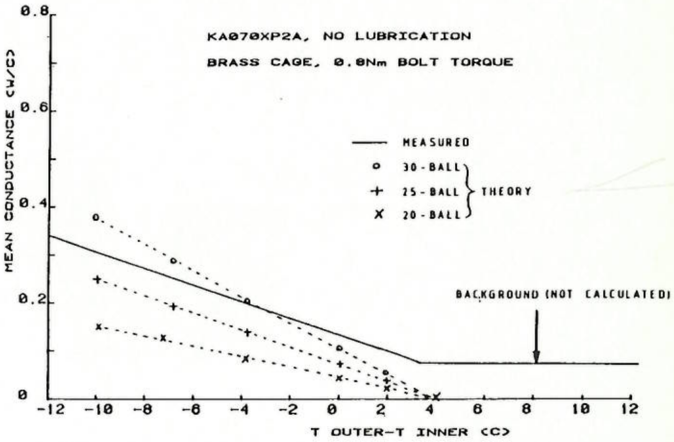

FIG 10 COMPARISON OF THEORETICAL AND MEASURED CONDUCTANCE

loading, Coulomb torque and dry thermal conductance.
Computing of ball speed and ball position variation in misaligned bearings can be valuable in warning of potential difficulties (or in interpreting existing ones!).
Since all the computing methods discussed depend upon simple regression formulae and straightforward iteration they are well within the capacity of many small desk machines.

Appendix

Formulae for calculation of Hertz constant, ellipse size etc.

The rigorous determination of the Hertz deflection constant and of the dimensions of the contact ellipse between a ball and a groove requires the evaluation of elliptic integrals. This is a time-consuming exercise, especially for small computers, but if only modest computational accuracy is adequate (eg. to 1 or 2 %) then it is better to make use of linear regression formulae. Very useful regression formulae are given by Brewe and Hamrock(1977). These formulae are as follows (see nomenclature):

Ratio of major to minor axes (ellipticity)

$$K = 1.0339 \left(\frac{R_y}{R_x}\right)^{0.636} \qquad \text{... A1}$$

Elliptic integral (first kind)

$$E1 = 1.5277 + 0.6023 \left(\frac{R_y}{R_x}\right) \qquad \text{... A2}$$

Elliptic integral (second kind)

$$E2 = 1.0003 + \frac{0.5968}{(R_y/R_x)} \qquad \text{... A3}$$

Where R_x ,R_y are the effective radii of curvature in the x,y principal planes (ie, longitudinally and transversely to the rolling direction).

From these expressions the Hertzian normal approach, δ_n (the elastic deformation at the contact centre) is given by:

$$\delta_n = \left\{\frac{9\,Q^2\,E1^3}{2\pi^2 E'^2 K^2 E2 R}\right\}^{1/3} \qquad \ldots \text{A4}$$

Thus the total normal approach for both ball contacts is:

$$\delta_n = \delta_{ni} + \delta_{no} = \left\{\frac{9\,Q^2}{2\pi^2 E'^2}\right\}^{1/3} \left[\left\{\frac{E1^3}{K^2 E2 R}\right\}_i^{1/3} + \left\{\frac{E1^3}{K^2 E2 R}\right\}_o^{1/3}\right] \qquad \ldots \text{A5}$$

where i and o refer to inner and outer raceway, respectively.

Defining the Hertz deflection constant, by:

$$K_n = Q/\delta_n^{3/2} \qquad \ldots \text{A6}$$

we then have:

$$K_n = \frac{\sqrt{2}}{3}\pi E' \left[\left\{\frac{E1^3}{K^2 E2 R}\right\}_i^{1/3} + \left\{\frac{E1^3}{K^2 E2 R}\right\}_o^{1/3}\right]^{-3/2} \qquad \ldots \text{A7}$$

The semi-major axis, a, of the ellipse of contact is:

$$a_{i,o} = \left\{\frac{6Q\,R\,K^2 E2}{\pi\,E'}\right\}_{i,o}^{1/3} \qquad \ldots \text{A8}$$

From this the maximum compressive stress in the contact is:

$$P_o = \left\{\frac{3\,Q\,K}{2\pi\,a^2}\right\}_{i,o} \qquad \ldots \text{A9}$$

These expressions are easily converted into program lines and can form a useful subroutine for many purposes.

Acknowledgement

Mr H M Briscoe and Dr R H Bentall of ESTEC have provided funding and encouragement for the work described here.
The author is grateful to the Managing Director, Northern Division, UKAEA for permission to publish.
Dr R A Rowntree, Mr K T Stevens and Mr R Watters of ESTL have given valuable assistance in the experimental measurements.
British Aerospace (BADG), Stevenage gave permission to describe the L-SAT SADM.

References

Harris T (1966) "Rolling bearing analysis" Wiley

Brewe D E and Hamrock B J (1977) "Simplified solution for elliptical contact deformation between two elastic solids" Trans. ASME Series F, 99,4.

Todd M J (1980) "A method for the calculation of torque in dry-lubricated ball bearings including the influence of temperature and fit" Proc. 2nd Space Tribology Workshop, ESTL (ESA SP-158).

Johnson K L (1962) "Tangential tractions and microslip in rolling contact" in "Rolling contact phenomena" Elsevier.

Tabor D (1955) "The elastic work in rolling a sphere on another surface" Brit. J Appl. Phys. 6, p79

Barish T (1969) "Ball speed variation in ball bearings and its effect on cage design" Lubr.Eng.

Jones A B (1960) "A general theory for elasticlly constrained ball and roller bearings under arbitrary load and speed conditions" J. Basic Eng.

Stevens K T and Todd M J (1980) "Thermal conductance across ball bearings in vacuum" ESA Trib/1

Rowntree R A (1983) "The stiffness, torque and thermal conductance of thin-section four-point contact ball bearings for use in spacecraft mechanisms" This symposium